European Polymer Journal 221 (2024) 113548

Contents lists available at ScienceDirect

European Polymer Journal

journal homepage: www.elsevier.com/locate/europolj

Pectin/Alginate bio-nanocomposite hydrogel beads based on in-situ formed layered double hydroxide in the presence of Mentha extract: Antibacterial carrier for potential pH-responsive targeted anti-cancer drug delivery

Roghayeh Fathi, Siamak Javanbakht, Reza Mohammadi *

Polymer Research Laboratory, Department of Organic and Biochemistry, Faculty of Chemistry, University of Tabriz, Tabriz, Iran

ARTICLE INFO

Keywords:
Pectin
Alginate
Layered Double Hydroxide
Mentha extract
Drug delivery
Antibacterial

ABSTRACT

This research presents the creation of novel pH-responsive drug delivery carriers with potential applications in cancer treatment. The study involved the Mentha Extract (ME) for the in-situ synthesis of Layered Double Hydroxide (LDH) bio nanoparticles (LDH-ME NPs). These NPs were incorporated into a biopolymeric hybrid formulation containing Pectin and Alginate to produce bio-nanocomposite hydrogel beads. The morphology and chemical composition were assessed and confirmed through various techniques. Doxorubicin (DOX) was employed as a representative anti-cancer medication to investigate the controlled drug release properties of the newly developed hydrogel beads (loading capacity: ~92 %). *In vitro* experiments revealed that the drug release pattern was significantly regulated in response to pH levels (with a higher drug release rate at pH 7.4, about 89 %). The assessment for antibacterial properties validated the effective antibacterial performance of the hydrogel beads toward *S. aureus* and *E. coli* with inhibition zones about 20 mm and 14 mm, respectively. MTT assay indicated a high level of cytocompatibility with HT-29 cells (cell viability exceeding 95 %) for the blank bio-nanocomposite hydrogel beads. Conversely, bio-nanocomposite hydrogel beads loaded with DOX exhibited notable cytotoxicity (~13 % cell viability in 15.6 μg/mL) against HT-29 cells. These findings recommend the current bio-nanocomposite as a promising bio-platform with superior antibacterial and anti-cancer properties.

1. Introduction

A hydrogel consists of a matrix of interconnected hydrophilic chains, creating a three-dimensional (3D) framework, which may be derived from natural or artificial polymers [1]. The exceptional ability of hydrogels to retain and absorb a diverse range of biological fluids, water, and solute molecules is attributed to their hydrophilic functional groups. These groups induce the hydrogels to expand up to tens of times their original dry weight [2]. Hydrogels have found application in various areas within the biomedical domain, such as cancer research, stem cell engineering, drug delivery, and tissue engineering, because of their environmental responsiveness, swelling/de-swelling behavior, biocompatibility, and many other electrical, physical, chemical, and biological features that mimic biological tissues [3–7]. Drug delivery benefits significantly from the frequent retention, capture, or release of materials via the 3D porous matrix of hydrogels [8]. Nevertheless, hydrogels' restricted functionality and mechanical qualities preclude further use in the biomedical industry [9]. In this context, the first nanocomposite hydrogels (NHs) demonstration occurred in 2002 [10]. Hydrogels have drawn a great deal of attention and investigation from researchers because of their strategy to integrate the advantageous properties of nanomaterials within their 3D networks. NHs, or three-dimensional molecular networks, are created when a polymer is covalently or physically cross-linked with nanostructures or nanoparticles [9]. Without a doubt, NHs make excellent carriers for medication delivery systems. The NH-based drug delivery systems can: 1) control the release profile of therapeutic agents by their distinct physical characteristics (i.e., diffusion coefficient, swelling ratio), 2) act as a library of bioactive molecules by way of interactions with hydrogel matrix or nano-partials, and 3) be in charge of the multi-stimulus (i.e., temperature, pH, magnetic field, and electric field), drug delivery response systems, 4) and enhancing synergies (i.e., photothermal conversion effect) to treat illnesses, deliver drugs precisely where they are needed, and more [11–14].

Bio-nanocomposites have attracted much attention due to their inherent properties, including improved structural and functional

* Corresponding author.
E-mail addresses: roghayeh.fathi@gmail.com (R. Fathi), siamakjavanbakht14@yahoo.com (S. Javanbakht), r.mohammadi@tabrizu.ac.ir (R. Mohammadi).

https://doi.org/10.1016/j.eurpolymj.2024.113548
Received 16 June 2024; Received in revised form 19 October 2024; Accepted 31 October 2024
Available online 13 November 2024

aspects, non-toxicity, flexibility, biocompatibility, and biodegradability [12,15,16]. Biopolymers are fascinating due to their renewability, low production costs, and diverse pharmaceutical uses [15,16]. Here, the drug is shielded from early release in the stomach and small intestine's acidic pH by using pH-sensitive polymers, which increase the amount of active ingredients in the colon area [17,18]. Because of their excellent biological performance, biocompatibility, and enzyme-controlled biodegradability, natural polysaccharides like cellulose derivatives, pectin, alginates, and natural gums continue to play an important role in the field of oral controlled-release dosage forms [17,19]. Pectin (PC), a heterogeneous anionic polysaccharide, is a natural polymer widely used in the food industry as a gelling agent, thickener, and stabilizer. Carboxyl groups attach to linearly connected a-(10/4)-D-galacturonic acid residues in this biopolymer. The structural properties of PC, such as its degree of esterification, can be modified to improve its performance as DDS. Furthermore, PC possesses significant promise for diverse biomedical applications given its unique attributes, including non-toxicity, accessibility, biodegradability, biocompatibility, hydrophilicity, pH sensitivity, outstanding chemical stability, capability to form gels, ease of modification, and limited solubility in organic solvents. Interestingly, PC has gained much attention as a carrier for colon targeting since it is almost entirely degraded by colonic bacteria [20]. Sodium alginate (ALG) is taking center stage as an ideal matrix for controlled drug delivery in the pharmaceutical industry. ALG is a polyelectrolyte and a natural polysaccharide derived from brown algae belonging to the Phaeophyceae. Its structure is composed of two monomeric units, β-D-mannuronic acid and α-L-guluronic acid. The ALG salts have the characteristic to form a uniform, transparent, water-insoluble, and thermo-irreversible gels hydrogel when they are in contact with di- or trivalent cations (i.e. Ca^{2+}, Fe^{2+}, Mn^{2+}, Al^{3+}) forming a reticulated structure due to ionic interaction between the ions and carboxyl group, mainly belonging to guluronic blocks. The interest in ALG is mainly due to the gel-forming properties and this characteristic has been exploited to fabricate beads as sustainable drug delivery systems [21,22]. One known major disadvantage of oral formulations based on single polysaccharides is the early release of the drug in the upper part of the gastrointestinal tract (GIT). It may be possible to prevent this release by carefully combining two or more polysaccharides [23–26]. Moreover, when needed, a multilayered system offers the capacity to deliver the medication to a specific region of the body or at a designated time of day, particularly for addressing severe chronic mucosal inflammations such as Inflammatory Bowel Disease (IBD) [17]. In recent years, new drug delivery systems have been developed based on bio-hybrid nanocomposites consisting of an inorganic phase as a dispersed phase and a natural polymeric matrix [27]. These nanocomposites are perfect as drug delivery systems because of their biocompatibility, biodegradation, inertness, ease of preparation, suitable mechanical strength, and capacity to load large volumes of different drugs [28]. Layered-double hydroxides (LDH) containing replaceable anions within pseudo-brucite cationic interlayers are a type of nanoparticle utilized in drug delivery applications. These particles have garnered significant interest for their ability to transport anionic drugs and various bioactive compounds to cells, owing to their minimal harm to targeted cells, compatibility with biological systems, strong durability, effective shielding of drugs from unwanted degradation, developed cellular uptake behavior, and pH-dependent dissolution [29,30]. Trivalent cations (M^{3+}), which give the brucite lattice a positive charge, replace a portion of the divalent cations (M^{2+}), giving rise to the LDH structure. Interlayer anions neutralized the generated positive charge and produced layers with thicknesses of several ten nanometers. [27]. The general LDH formula is written as $[M^{II}_{1-x}M^{III}_{x}(OH)_2]^{X+}(A^{n-})x/n \cdot yH_2O$, in which M^{II} are divalent metal cations such as Ca^{2+}, Mg^{2+}, and Zn^{2+}, M^{III} are trivalent metal cations like to Fe^{3+}, Ga^{3+}, Al^{3+} and A^{n-} are CO_2^{3-}, Cl^- or NO^{3-} anions as well as x is usually a range between 0.2 and 0.4. The majority of the techniques for producing LDH involve hydrothermal synthesis, regeneration, ion exchange, and co-precipitation of inorganic salts in basic solution at low and high supersaturation states [31,32]. The presence of LDHs usually improves drug transport without modifying the chemical structure and the pharmacological activity. Moreover, it is known that the intercalation of a drug in LDH structure determines a multistep release process characterized by an initial rapid release followed by a slower step, usually related to anionic exchange with anions of the medium [21].

Plant extracts are considered diverse biological resources with the quality of safety, easy access, compatibility with living organisms, and the ability to regulate resistance and structure effectively. The antioxidants present in plant products will protect the body from free radicals and thus prevent cancer. In this context, Peppermint, Mentha piperita (M. piperita), Lamiaceae family, one of the most important medicinal plants in traditional medicine, can be used as a natural anticarcinogenic drug for treating cancer. The extract of M. piperita leaves contains flavonoids and phenolic acids and also the essential oil of M. piperita contains acetaldehyde, amyl alcohol, Pulegone, menthyl esters, phellandrene, limonene, pinene, dimethyl sulfide, alpha- and beta-thujone, citronellol, menthol, menthone, menthofuran, alpha-pinene, sabinene, ocimene, gamma-terpinene, terpinolene, iso menthone, menthyl acetate, and other compounds which are capable of providing the above-mentioned effects [33]. The chemical structure of the main flavonoids of ME is provided in Fig. S1 [34,35].

The main objective of this work is to create a range of multi-stimulus responsive hydrogel beads using nanocomposite materials that can simultaneously respond to temperature and pH changes. For this purpose, Mentha extract was utilized for the green and in-situ synthesis of Al/Zn LDH NPs, leveraging its high antioxidant properties. Subsequently, LDH-ME bioNPs were incorporated into a hybrid hydrogel composed of biopolymers (i.e., PC and ALG) due to their excellent compatibility and potential to facilitate targeted drug delivery to the lower part of the digestive tract. This innovative approach aims to enhance the biosynthesis process of the hydrogel beads for nanocomposite materials. The hypothesis driving this research posits that integrating LDH-ME bioNPs will significantly improve the controlled release of DOX, a model drug, at specific pH levels, thereby offering a promising avenue for targeted cancer treatment through these novel drug delivery systems. On the other hand, a green method for the in-situ synthesis of LDH nanoparticles in the presence of Mentha plant extract, compared to previous works, triggers the synergistic effect of several bioactive features, including antibacterial, antioxidant and anti-cancer properties, was investigated and confirmed. As far as we know, most reported similar works are dedicated to one or two bioactive properties in one platform in the literature [20,21,36–38]. The results obtained from this study will provide insights into the efficacy of these systems in achieving enhanced therapeutic outcomes.

2. Materials and methodologies

2.1. Materials

Mentha plant (Tabriz-Iran), Alginate (Mw = 110 kDa and DD=84 %), and Pectin (55–70 % esterified and Mw > 100 kD) were purchased from Sigma Aldrich and Food chem Co. Doxorubicin (DOX) were purchased from Sobhan Pharmaceuticals Co. (Iran). $Al(NO_3)_3 \cdot 9H_2O$, and $Zn(NO_3)_2 \cdot 6H_2O$, NH_3 (25 %) were obtained from Merck Co. All other chemicals without any purification with analytical grade were used.

2.2. Synthesis of LDH bio nanoparticles (LDH-ME NPs)

The Mentha plant was grown locally in Tabriz, Iran, and its leaves were harvested. Before being processed into Mentha Extract (ME), the leaves were cleaned of dust using tap water. Using the Soxhlet extraction method, 30 g of Mentha leaves were extracted with 150 mL of methanol [39]. Whatman No. 41 filter paper was used to filter the resulting crude extract to eliminate any particles. Following filtration, a rotary

evaporator was used to fully evaporate the particle-free crude extract, which was then stored at 4 °C.

The co-precipitation technique was used in an alkaline environment to prepare Al/Zn LDH [40]. In brief, $Al(NO_3)_3{,}9H_2O$ (33.50 mmol) and $Zn(NO_3)_3{\cdot}6H_2O$ (16.50 mmol) were dissolved in bi-distilled water (50 mL). Then, this solution was added to 20 mL of the Mentha Extract (ME, 2 % w/v), and NaOH solution (2 M, 40 mL) was added dropwise to the metal ions containing solution with constant stirring under the N_2 atmosphere. The reaction was continued at 95 °C for 24 h while the pH was kept at 9–10 with NaOH solution. To remove impurities and adjust pH, the resulting mixture was washed three times with bi-distilled water. Finally, the synthesized LDH-ME NPs were dried for 24 h at 50 °C in a vacuum oven.

2.3. DOX loading in LDH-ME NPs

According to the reported method [1], to load the drug, first LDH-ME NPs were added to DOX stock solution (20 ml, 100 ppm) and dispersed in an ultrasonic bath (Elma sonic Easy 60H, Germany) for 10 min, and then for 72 h was shaken at ambient temperature using a shaker to reach equilibrium. Then, it was centrifuged, and the supernatant was collected in the next step. After washing the drug that had been adsorbed on the surface, DOX-loaded LDH-ME NPs were vacuum-dried at room temperature. Using UV–Vis spectroscopy, the amount of DOX loading in the collected supernatant was determined. The amount of unloaded DOX was determined (ppm) by converting the UV–Vis absorption of the supernatant to a concentration using the calibration curve of DOX. The amount of loaded DOX was obtained by deducting the unloaded DOX amount from the initial DOX amount. The amount of drug loading capacity (DLC) was calculated using Eq. (1).

$$DLC\% = \frac{(\text{Amount of drugs in carrier (mg)})}{(\text{Initial amount of drugs (mg)})} \times 100 \quad (1)$$

2.4. Encapsulation of DOX-loaded LDH-ME NPs with PC/ALG biopolymers and preparation of nanocomposite hydrogel beads

Hydrogel bead formation procedure [17] was used to encapsulate DOX-loaded LDH-ME NPs with PC/ALG biopolymers. Briefly, the PC/ALG biopolymers solution was prepared by adding 500 mg of PC and 500 mg of ALG in 15 mL of bidistilled water. The DOX-loaded LDH-ME NPs solution (0.3 g in 50 mL) was dropwise added into the PC/ALG biopolymers solution and the mixture was stirred at room temperature for 2 h to reach a homogenous mixture. In the following, by dropwise addition of the prepared mixture to the $CaCl_2$ solution (2 % w/v), DOX-loaded LDH-ME NPs@PC/ALG hydrogel beads were formed. To get rid of the unreacted $CaCl_2$ from the bead surface, the beads were filtered and treated three times with bi-distilled water. The resultant hydrogel beads were then dried for 24 h at 50 °C in a vacuum oven.

The DOX-loaded nanocomposite hydrogel beads (DOX-loaded LDH-ME NPs@PC/ALG) were removed from the solution, and the supernatant was used to assess the DLC utilizing a UV–Vis spectrophotometer at $\lambda_{max} = 480$ nm according to the Eq. (1).

2.5. Drug release study

To study *in-vitro* drug release, 20 mg of the DOX-loaded LDH-ME NPs@PC/ALG were immersed into 10 mL of buffered solutions (pH 1.2, 6.8, and 7.4 phosphate buffer) and kept at 37 °C in a shaker incubator. 2 mL of the solution was taken out at predetermined intervals to determine the amount of the released DOX in the media. An equivalent buffer solution was added to the released media to reserve the lost volume constant. Using calibration curves for DOX, the amount of released DOX was measured at $\lambda_{max} = 480$ nm with UV–Vis. The percentage cumulative release (CR, %) of the drug from the hydrogel beads was determined using Eq. (2).

$$CR(\%) = \frac{(10Cn + 2.0\Sigma Cn - 1)}{M_0} \times 100 \quad (2)$$

The value of n denotes the number of steps taken to withdraw the releasing media, where C_n and C_{n-1} indicate the drug concentrations (mg/L) after the n-th and n-1th withdrawing steps correspondingly. Moreover, M_0 signifies the amount of drug (mg) initially placed within the hydrogel beads. The 10 to 2 ratio is utilized to determine the concentration of DOX by accounting for the eliminated volume [35].

Moreover, several kinetic models are fitted to the release profile [41], which are compiled in Table 1; in light of this, the release kinetics were evaluated. Every guideline is calculated using linear regression.

2.6. In-vitro swelling and erosion determination

The in-vitro swelling and erosion behaviors of the DOX-loaded LDH-ME NPs@PC/ALG hydrogel beads were tested in PBS, pH 1.2, 6.8, and 7.4. The samples (about 10 mg) were pre-weighed and followed by immersed in 10 mL of buffered solution. The swollen beads were taken out at specified intervals and weighed after blotting with filter paper to remove surface water. Weight gain and weight loss were considered as swelling and degradation, respectively [42]. The swelling percentage and erosion percentage were calculated with Eq. (3) and (4):

$$Swelling(\%) = \frac{Ws - Wi}{Wi} \times 100 \quad (3)$$

$$Erosion(\%) = \frac{Wi - Wd}{Wi} \times 100 \quad (4)$$

Where Wi, Ws, and Wd are the weights of the initial, swollen, and dry samples, respectively.

2.7. Antioxidant assay

The DPPH free radical scavenging activity of LDH-ME NPs@PC/ALG nanocomposite hydrogel beads was evaluated according to the reported procedure with slight modifications. Briefly, various concentrations (1–15 μg/mL) of nanocomposite hydrogel beads were exposed to 1 mL of DPPH radical ethanolic solution (25 ppm) and vigorously shaken in the dark at room temperature for 60 min. The UV–Vis absorbance of the samples was recorded at 517 nm against an ethanol blank. The antioxidant effectiveness of the samples was quantified as a percentage of DPPH radical inhibition using the following Eq. (5) [43].

$$\text{Inhibition}\,(\%) = (A_{control} - A_{sample})/\text{Acontrol} \times 100 \quad (5)$$

$A_{control}$ is the value of the DPPH absorbance, and A_{sample} is the absorbance value of the test solution.

2.8. Antibacterial activity

The antibacterial behavior of the LDH-ME NPs@PC/ALG hydrogel beads toward *Escherichia coli* (*E. coli*, ATCC 25922) as Gram-negative bacteria and *Staphylococcus aureus* (*S. aureus*, ATCC 25993) as Gram-positive bacteria were evaluated by the disc diffusion method [38]. To

Table 1
The result of fitting the DOX release profile from nanocomposite hydrogel beads at pH 7.4 with different kinetics models.

Kinetic models	Equations	R^2
Zero-order	$F=k_0t$	0.57
First-order	$\ln(1-F) = k_f t$	0.559
Higuchi	$F=k_H\sqrt{t}$	0.754
Weibull	$\ln[-\ln(1-F)] = -\beta\ln t_d + \beta\ln t$	0.988

k_0, k_f, and k_H are the kinetic constants of respective models and F is the fraction of drug released up to time t.

achieve this, spore suspensions of bacteria (50 μL containing 1 × 10^4 cells/mL) were used to infect the agar plates. After that, the hydrogel beads were put on top of the agar. The plates were kept at 37 °C for the entire night. After that, a ruler was used to determine the diameter inhibitory zones' appearance.

2.9. MTT cell viability

The cytotoxicity of free DOX, LDH-ME NPs@PC/ALG nanocomposite hydrogel beads, and DOX-loaded LDH-ME NPs@PC/ALG nanocomposite hydrogel beads toward HT-29 cells were investigated by using the MTT assay [37]. First, HT-29 cells were cultured in 96-well plates with 100 μL of full media in each well. The cells were then incubated for 24 h at 37 °C with carbon dioxide gas present. Each well received 100 mL of new complete media and different sample dilutions (1.25–20 μg/mL) after removing the culture medium. Each well was then incubated for 48 h at 37 °C in a dark environment. The MTT reagent (20 mL, 5.0 mg/mL) was then added to the wells, and they were left at a dark station for 4 h. After carefully removing the remaining MTT solution from each well, 150 μL of DMSO was added in its place. The absorbance of each well was measured using a microplate reader that was calibrated to 570 nm. The three replicates' mean was also shown in the cultivation tests. The percentage of cell viability was calculated by using Eq. (6):

$$Cellviability(\%) = \frac{(Reactedcells)}{(opticaldensityofthecontrol)} \times 100 \quad (6)$$

Here, the terms "reacted cells" and "control" refer to the optical densities of the treated and control cells containing samples, respectively.

3. Results and discussion

The utilization of biomaterials has become a prevalent method for enhancing the viability of biomedical platforms in recent times. The current investigation introduces a novel carrier constructed from biopolymers (i.e., PC and ALG) along with LDH-ME NPs, chosen for their attributes such as biocompatibility, biodegradability, and cost-effectiveness. Subsequently, following the extraction of antioxidant/phenolic compounds from the Mentha plant, LDH NPs were fabricated in the presence of ME. Subsequently, to facilitate the encapsulation of DOX within LDH-ME NPs, they were dispersed in a DOX solution and agitated

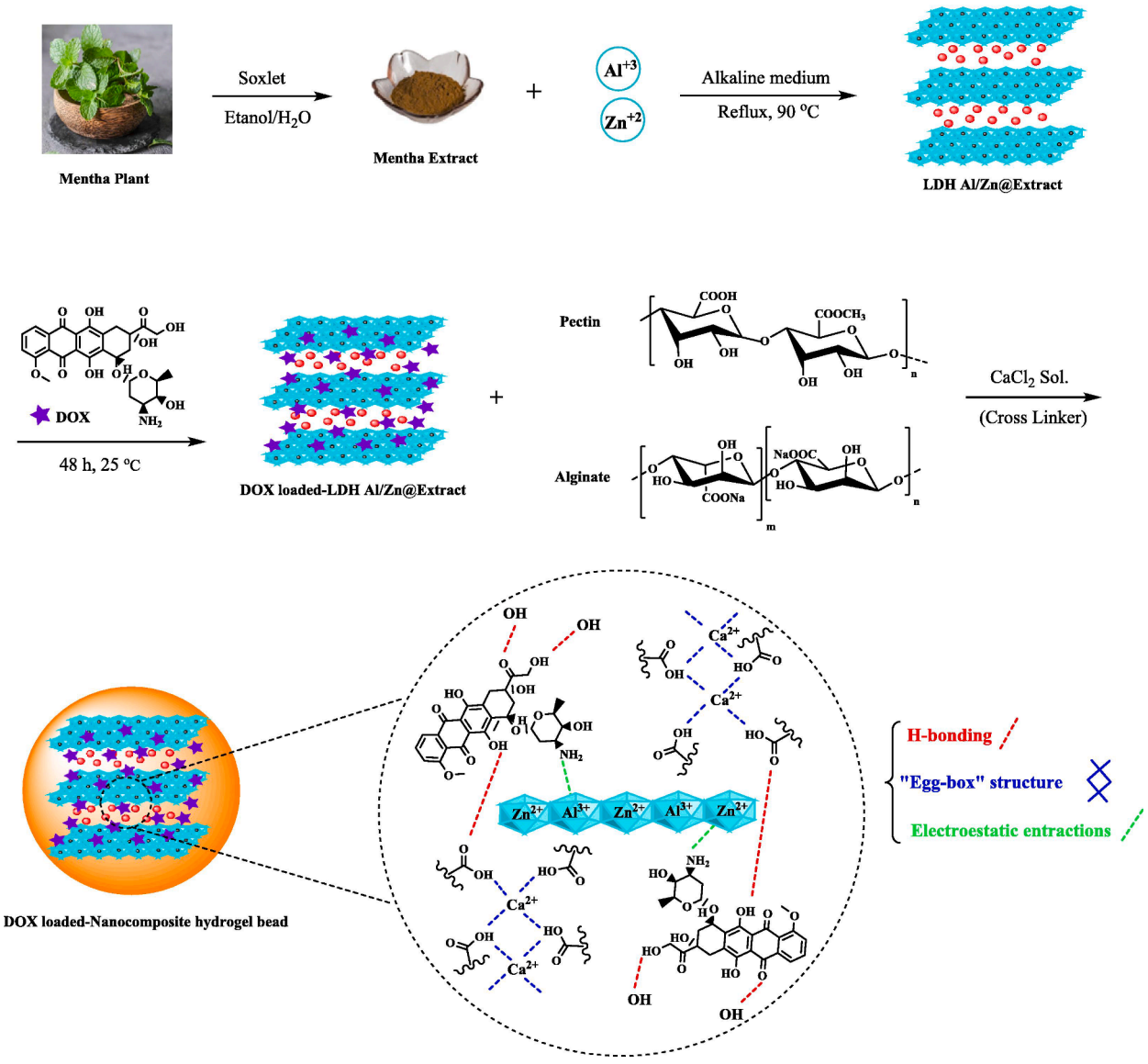

Scheme 1. Preparation of ALG/PC-encapsulated DOX loaded-LDH-ME NPs nanocomposite hydrogel beads.

at ambient temperature for 72 h. The supernatant was collected after centrifuging the mixture in the next step. Subsequently, DOX-loaded LDH-ME NPs were synthesized and interacted via hydrogen bonding with a blend of PC/ALG biopolymers via hydroxyl and carboxylic acid groups. Ultimately, the mixture was dropped to the $CaCl_2$ solution to form hydrogel beads. The carboxylic acid and hydroxyl groups form hydrogen bonds, which allow ALG and PC to interact. On the other hand, the electrostatic interactions between DOX and LDH ions, as well as the interaction of carboxylate groups on biopolymers with Ca^{2+}, Al^{3+}, and Zn^{2+} ions within LDH layers, lead to the formation of the final hydrogel nanocomposite structure. The carboxylate groups on PC and ALG form an "egg-box" structure through Ca^{2+} ions, which leads to a homogenous hydrogel between pectin and alginate biopolymers. (i.e., coordination with Ca^{2+} ions) [44–46]. This structure can prevent the early release of the drug in the upper part of the GIT thanks to the presence of ALG resistant to the stomach and its delivery specifically in the large intestine due to the selection of PC for this area. Therefore, this hydrogel nanocomposite can be useful for the selective and gradual delivery of drugs to the colon [17]. A schematic of the DOX-loaded LDH-ME NPs@PC/ALG nanocomposite hydrogel beads is presented in Scheme 1.

3.1. Characterization of synthesized materials

3.1.1. FT-IR study

FT-IR spectra were obtained for ME, PC, ALG, LDH NPs, LDH-ME NPs, and the synthesized nanocomposite hydrogel beads (Fig. 1A). Within the ME spectrum, the stretching vibration bands corresponding to C-O–H and C-O functionalities are observed at 1070 cm^{-1} and 1263 cm^{-1}, respectively. The active methylene flexion manifests as a series of sharp, intense bands at 1384 and 1451 cm^{-1}. A notable characteristic of the C=O group is the prominent peak at approximately 1614 cm^{-1}. The peaks at 2857 cm^{-1} and 2925 cm^{-1} are attributed to the C–H stretching of the methyl group, whereas the strong and broad peak at 3422 cm^{-1} is associated with the O–H stretching vibration. (Fig. 1A (a)) [35]. The FT-IR spectrum of pure PC had the bands at 3341, 2931, 1735, 1607, and 1438 cm^{-1}, which related to the vibrations of O–H stretching, C–H stretching, C=O stretching (in $–COOCH_3$), −COO asymmetric stretching, and − COO symmetric stretching (Fig. 1A (b)) [20]. In the ALG spectrum, the absorption band located within the range of 3400–3600 cm^{-1} is ascribed with the O–H bonded group, while the stretching vibration bands of C–H are observed at 2921 and 2875 cm^{-1}. Moreover, the peak present at 1674 cm^{-1}, along with the discernible peaks ranging from 1010 to 1200 cm^{-1} are denoted as the stretching vibration of the C=O, C-O, and C-N groups, respectively (Fig. 1A (c)) [47]. The stretching vibrations of the lattice water and –OH groups appeared as strong overlapping bands at 3480 and 3636 cm^{-1} in the LDH NPs spectrum. The H–O–H bending vibration of water molecules in the interlayer of LDH NPs was identified as the cause of the peak at 1620 cm^{-1} (Fig. 1A (d)) [48]. In the LDH-ME NP_S spectrum, the appearance of the peaks related to the stretching vibrations of C=C and O–H bonds at 1300–1500 cm^{-1} and 3200–3600 cm^{-1}, respectively, confirms the successful synthesis of LDH NPs on the plant extract. Also, an increase in the intensity of all peaks is detected compared to the spectrum of LDH NP_S, which is owing to the interactions between LDH NPs and the functional groups of ME (Fig. 1A (e)) [49]. In the spectrum of nanocomposite hydrogel beads (LDH-ME NP_S@PC/ALG), it can be mentioned that the diminish in the intensity of peaks compared to PC and ALG peaks along with the shifting of characteristic bands is owing to the interactions between ME and biopolymers (Fig. 1A (f)).

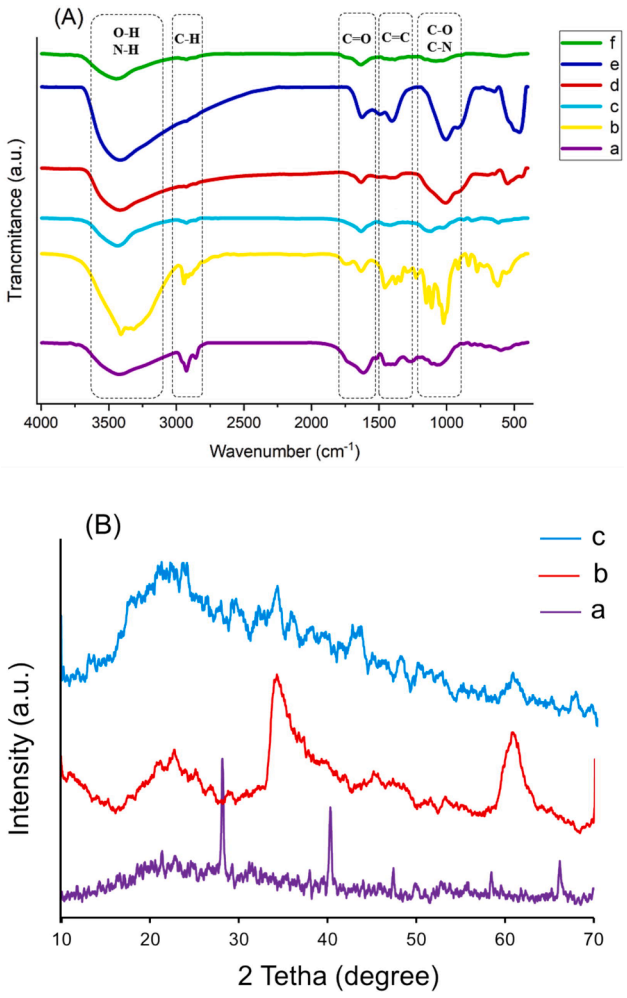

Fig. 1. (A) FT-IR spectra of ME (a), Pectin (b), Alginate (c), LDH NP_S (d), LDH-ME NP_S (e), LDH-ME NP_S @*PC*/ALG (f) and (B) XRD spectra of ME (a), LDH-ME NP_S (b), LDH-ME NP_S @*PC*/ALG (c).

3.1.2. XRD study

Powder XRD was used to characterize the formation of LDH-ME NPs and their subsequent presence in hydrogels (Fig. 1B). The XRD pattern of pure ME showed diffraction peaks at 2θ of 28.10°, 40.28°, 47.40°, and 66.16° (Fig. 1B (a)). The XRD pattern of the as-synthesized LDH NPs reveals the characteristic diffractions at 2θ values of 10.70°, 23.20°, 32.10°, 34.90°, 37.35°, 47.61°, 57.22°, 64.30°, and 69.7° which could correspond to their crystalline structure [35]. In addition, in the XRD pattern of LDH-ME NPs the detected broad diffraction peaks at 2θ = 23.10°, 35.70° and 62.90° show that LDH NPs were monotonously synthesized on the ME (Fig. 1B (b)) and in the XRD diffraction pattern of the LDH-ME NPs@PC/ALG, a detected broad peak at 2θ = 10-30° is attributed to the amorphous structure of PC/ALG biopolymers that is a typical peak for many hydrogels based on polysaccharide (Fig. 1B (c)). Moreover, according to the Scherrer equation (supporting information), the crystallite size of the LDH-ME NPs and LDH-ME NPs@PC/ALG was calculated to be 0.247 nm and 0.118 nm, respectively. This small crystallite size of LDH-ME NPs and LDH-ME NPs@PC/ALG can probably be related to the exfoliation of LDH NPs in the amorphous matrix.

3.1.3. Morphological studies

The SEM method was utilized to characterize the surface morphology of the hydrogel beads made from bio-nanocomposite materials (Fig. 2 A). As depicted in Fig. 2 A (a), the surface morphology for ME exhibits a nearly smooth appearance. On the other hand, the layered structure in the morphology of LDH NPs suggests that they are present on the ME's surface. (Fig. 2 A (b)). Fig. 2 A (c) shows the spherical structure of nanocomposite hydrogel beads after encapsulation of LDH-ME NPs with hybrids of PC/ALG biopolymers. The morphology of LDH-ME NPs on the surface of beads at varying magnifications is displayed in Fig. 2 A (d,e). As can be observed in the figures, the LDH-ME NPs have

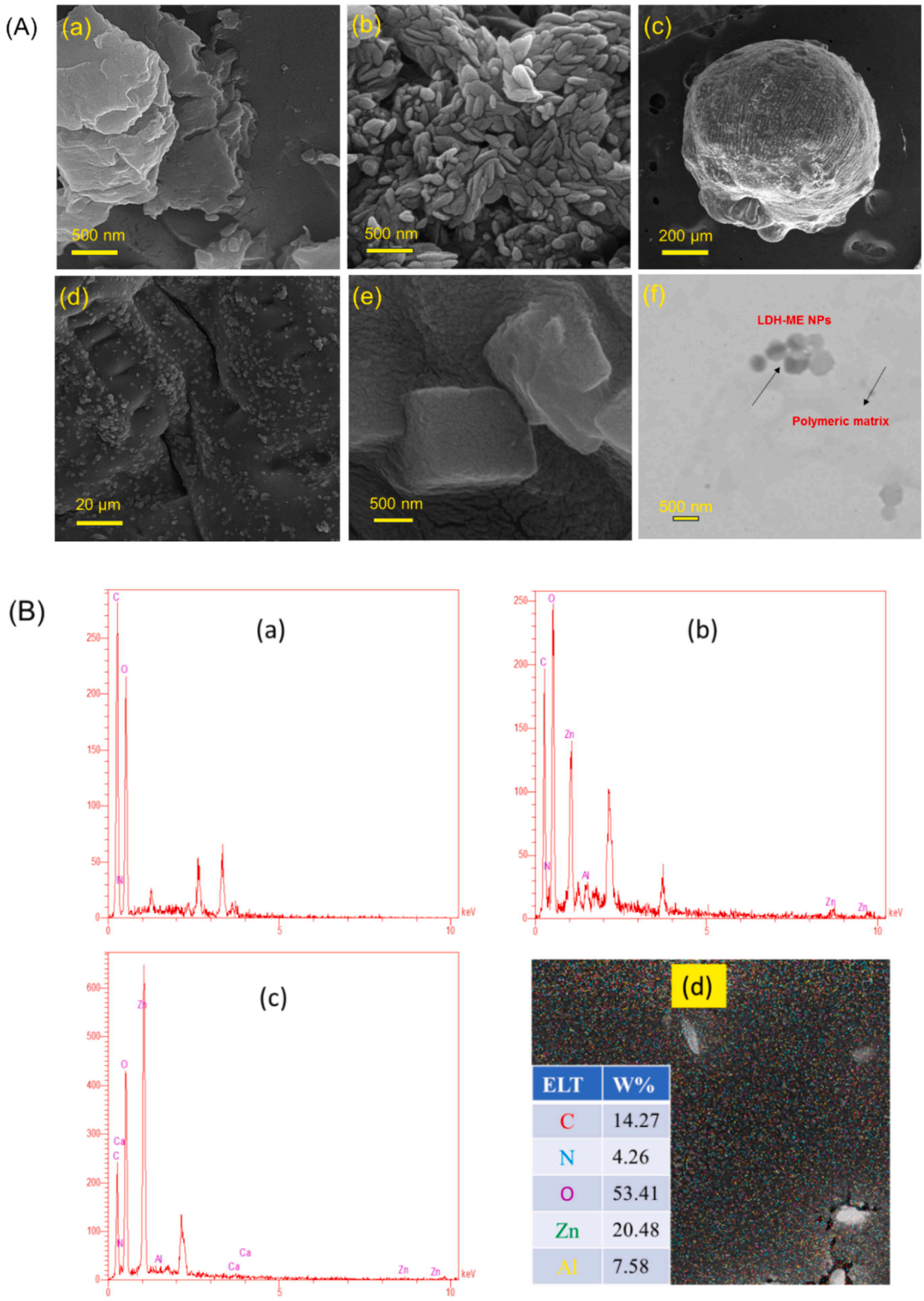

Fig. 2. (A) SEM micrographs of ME (a), LDH-ME NP_S (b), LDH-ME NP_S@ PC/ALG nanocomposite hydrogel bead (c, d, e), TEM of LDH-ME NPs@ PC/ALG (f), and (B) EDX spectra of ME (a), LDH-ME NPs (b), LDH-ME NPs @ PC/ ALG (c), and Mapping image of LDH-ME NPs (d).

the appropriate dispersion, verifying the existence of LDH-ME NPs in the PC/ALG biopolymeric network hybrids. Furthermore, the TEM image of the LDH-ME NP_S@ PC/ALG revealed the presence of LDH-ME NPs with a homogeneous distribution in the bio-polymeric PC-ALG matrix (Fig. 2 A (f)).

3.1.4. *EDX analysis*

Using the EDX method, the elemental analysis of synthetic samples was examined (Fig. 2 B). The presence of the Al and Zn elements in the EDX pattern of LDH-ME NPs compared with ME (Fig. 2 B (a)) revealed the successful synthesis of these NPs (Fig. 2 B (b)). Also, the increase in the peak intensity of carbon, nitrogen, and oxygen atoms and the

presence of Ca in the spectrum of LDH-ME NP_S@ PC/ALG nanocomposite hydrogel beads compared to LDH-ME NP_S confirms the successful formation of nanocomposite hydrogel beads (Fig. 2 B (c)). Besides, the Mapping image of LDH-ME NP_S shows the existence of Al, Zn, C, O, and N atoms with suitable dispersion in various weight percent (Fig. 2 B (d)).

3.1.5. Swelling and erosion studies

Since it is crucial in regulating the drug release of the carrier, the pH-sensitive swelling behavior of hydrogels is significant in drug delivery applications. Understanding how pH affects hydrogel integrity is vital for designing formulations that optimize drug release in targeted environments, such as the gastrointestinal tract, where varying pH levels are encountered. The swelling ratio is affected by ionic strength, temperature, pH, composition, and degree of cross-linking [36]. In this study, swelling studies of nanocomposite hydrogel beads were performed at pH 1.2, 6.8, and 7.4. (Fig. 4). The results demonstrate that the swelling behavior of nanocomposite hydrogel beads is time- and pH-dependent, peaking at pH 7.4. Lower swelling ratios arise from the non-occurrence of carboxylic acid functional groups deprotonation in the PC and ALG biopolymeric networks at pH 1.2. These circumstances led to the generation of H-bonding interactions between carboxylic acid groups, which caused the hydrogel to shrink. However, the carboxylic groups of PC and ALG were deprotonated at pH 7.4. Consequently, there has been increased swelling and electrostatic repulsion between carboxylate anions. As a result, hydrogel beads' ability to form hydrogen bonds between PC/ALG functional groups and water molecules allows them to absorb more water.

The findings from the erosion study indicate that hydrogel beads exhibit a reduced rate of weight loss in buffer media with a pH of 1.2, attributed to the preservation of structural integrity at this acidic level. As the pH increases to 6.8 and 7.4, the interaction of phosphate moieties in the buffered media with the hydrogel network leads to the degradation of essential physical cross-linking, particularly the COO-$Ca2^+$ interactions that maintain the hydrogel's stability [20]. This pH-dependent behavior is significant, as it influences both swelling and drug release profiles for applications in drug delivery systems. At lower pH levels, carboxyl groups within the hydrogel remain predominantly protonated, resulting in lower swelling and enhanced stability; conversely, higher pH levels ionize these groups, causing electrostatic repulsion that disrupts the cross-linked structure.

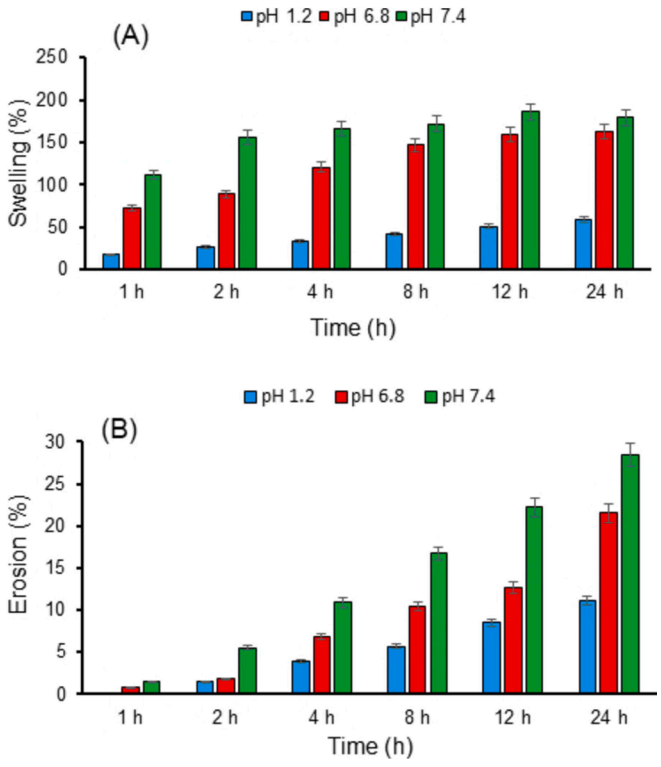

Fig. 3. Swelling (A) and erosion (B) percentages of LDH-ME NP_S@ALG/PC nanocomposite hydrogel beads at pH 1.2, 6.8, and 7.4.

3.1.6. Antioxidant study

The DPPH method was used to investigate the antioxidant activity of the LDH-ME NP_S@PC/ALG nanocomposite hydrogel beads. The results are shown in Fig. 4 a, b, and c. As illustrated in Fig. 3b, the DPPH peak intensity at 517 nm diminishes as the concentration of the nanocomposite hydrogel beads increases [50]. There was a correlation between the heightened antioxidant performance and the decreased absorption of the samples, indicating a dose-dependent relationship with the nanocomposite hydrogel beads. Fig. 3c shows the % radical scavenging activity of the nanocomposite hydrogel beads. The findings indicate that the nanocomposite hydrogel beads display remarkable antioxidant properties. The enhanced antioxidant activity observed for the nanocomposite hydrogel beads can be attributed to the redox property of ME extract [33]. This redox behavior allows ME extract to participate effectively in electron transfer processes, which is crucial for scavenging free radicals. According to Fig. 3c, the antioxidant activity of the synthesized hydrogel nanocomposite was slightly lower than the standard ascorbic acid.

3.1.7. DOX loading and release studies

The chemical structure of the carrier and drug has a significant role in the drug loading capacity. The high DOX loading (about 92 %) in the prepared carrier can be due to the layered structure of LDH-ME NPs and its high surface-to-volume ratio, interactions between the DOX and LDH-ME NPs (i.e., ion exchange and electrostatic interactions), which improve the loading efficiency of the drug. The rate of DOX released from the LDH-ME NPs@PC/ALG nanocomposite hydrogel beads at pH 1.2, 6.8, and pH 7.4 at 37 °C was considered by calculating the drug concentration using the UV–vis. Fig. 5 displays the profile of DOX release from hydrogel beads with respect to pH. Also, the increase in cross-linking density causes the reduced pore size, which has a key effect on the rate of drug release from the hydrogel beads. For instance, at pH 7.4, during 96 h about 89 % of the loaded DOX was released. On the other hand, the released rate significantly reduced at pH 1.2 (<25 % for DOX). The lower release rate of drug from hydrogel beads in pH 1.2 compared to pH 7.4, can be due to the stronger hydrogen bond in the acidic media and low swelling rate of the hydrogel network of pectin and alginate biopolymers. Increasing drug release at alkaline pH is related to the deprotonation of carboxylic acid groups of PC and ALG. In an alkaline environment (pH 7.4), PC and ALG cross-linked chains are destroyed due to the electrostatic repulsion. Alternatively, the carboxylate groups on PC and alginate form an "egg-box" structure through Ca^{2+} ions, which leads to a homogenous hydrogel between pectin and alginate biopolymers. (i.e., coordination with Ca^{2+} ions) [44–46]. Probably, with the increase in pH, the interaction of phosphate moieties in the buffered media (pH 7.4) with the hydrogel network leads to the degradation of physical cross-linking (i.e., egg-box structure), particularly the COO-Ca^{2+} interactions that maintain the hydrogel's stability ref, and accordingly releasing a higher DOX into the environment [20].

One of the best ways to anticipate drug release mechanisms is to research drug release kinetics. In this study, the release mechanism of DOX from hydrogel beads was predicted using the Zero-order, First-order, Weibull, and Higuchi models [36,41]. The Weibull distribution, which displays a continuous probability distribution, is the most suitable modeling candidate for releasing DOX from the profile of LDH-ME NPs@PC/ALG nanocomposite hydrogel beads (Table 1).

3.1.8. The antibacterial assessment

The present investigation utilized *S. aureus* and *E. coli* as

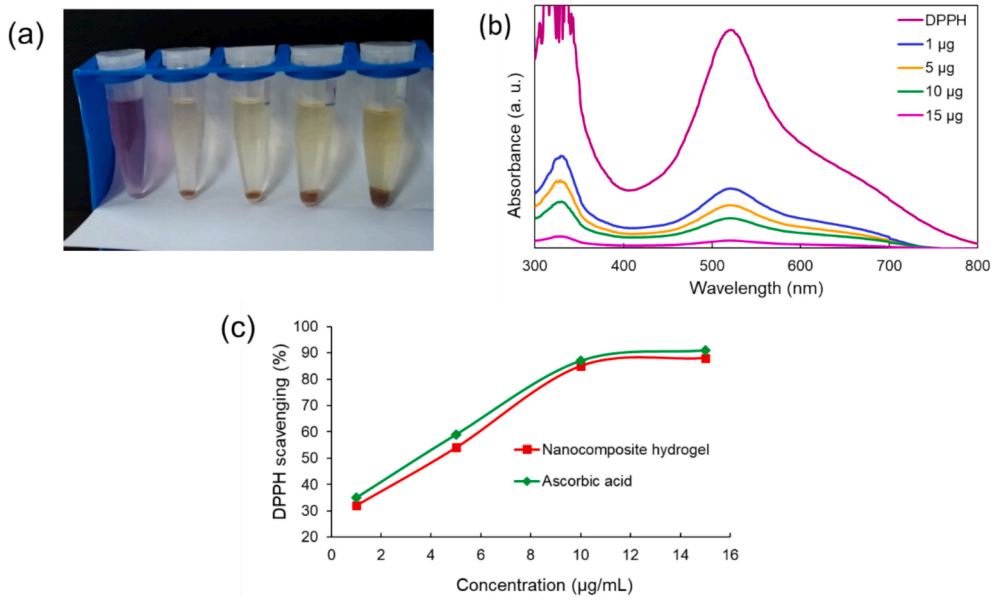

Fig. 4. Photograph illustrating the antioxidant activity (a), DPPH scavenging by LDH-ME NP_S@PC/ALG nanocomposite hydrogel beads (b), and UV–Vis spectra of nanocomposite hydrogel beads in 1–15 μg/mL concentrations to assess the antioxidant activity with DPPH assay (c).

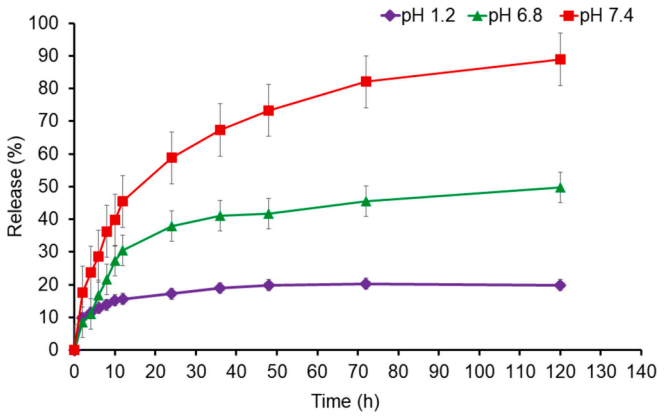

Fig. 5. DOX release profiles from LDH-ME NP_S@PC/ALG nanocomposite hydrogel beads at pH 1.2, 6.8, and 7.4 at 37 °C for 120 h. Result as means ± standard deviations (n = 3).

representative bacterial strains within the framework of a research inquiry. The assessment of the antibacterial properties inherent in the LDH-ME NPs@PC/ALG nanocomposite hydrogel beads was conducted utilizing the agar disc diffusion method, as illustrated in Fig. 6. The diameter of the inhibition zone surrounding the nanocomposite hydrogel beads was determined to be 14 mm for *E. coli* and 20 mm for *S. aureus*. Consequently, the nanocomposite hydrogel beads exhibited antibacterial activity toward both gram-negative and positive bacterial strains, displaying a slightly greater potency against *S. aureus* compared to *E. coli*. The compound ME exhibits antibacterial properties, which were further heightened through the incorporation of LDH NPs in combination with PC and ALG biopolymers. Conversely, this occurrence may be interpreted as a collaborative impact targeting bacterium. Hence, the LDH-ME NPs@PC/ALG hydrogel beads could be recommended as a viable antibacterial framework for addressing infectious ailments caused by bacteria.

3.1.9. *Cytotoxicity study*

The MTT analysis was employed to assess the cytotoxicity of the LDH-ME NPs@PC/ALG hydrogel beads. The findings illustrated a dose-dependent relationship in the cytotoxicity towards HT-29 cells. Fig. 7A indicated that the blank LDH-ME NPs@PC/ALG nanocomposite

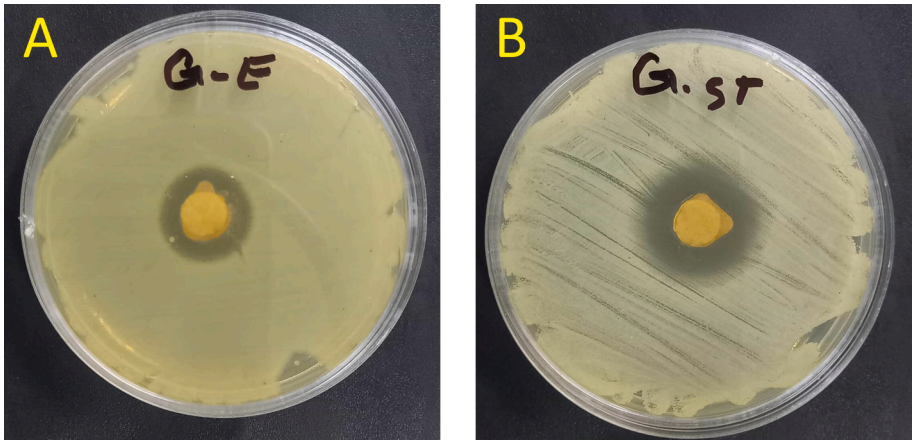

Fig. 6. The growth pattern of *E. coli* (A) and *S. aureus* bacteria (B) in the presence of LDH-ME NP_S@PC/ALG nanocomposite hydrogel beads.

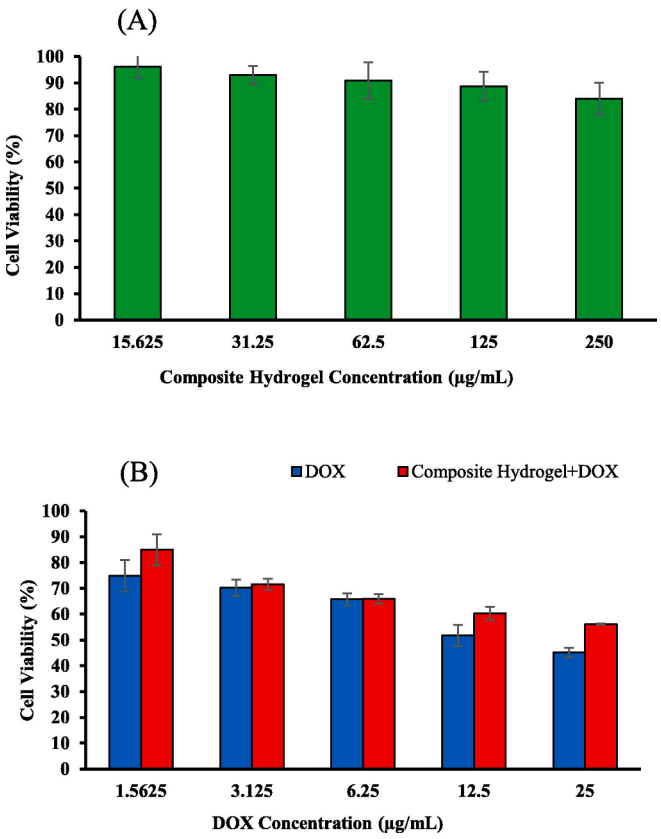

Fig. 7. *In vitro* cell viabilities of HT-29 cell lines after being incubated with various concentrations of LDH-ME NP_S@PC/ALG (A) and DOX-loaded LDH-ME NP_S@PC/ALG nanocomposite hydrogel beads and free DOX solution for 48 h (B). values shown are means ± standard deviations (n = 3).

hydrogel beads exhibited minimal cytotoxicity towards HT-29 cells following a 48-hour incubation period (90 % cell viability at 62.5 µg/mL). This is due to the use of biomaterials (i.e., ME, PC, and ALG) in the formulation of the synthesized nanocomposite. Consequently, it could serve as a safe carrier for delivering anti-cancer drugs. According to Fig. 7B, the higher concentration of the active drug results in increased cytotoxic effects. Free DOX exhibited higher cytotoxicity than that of DOX-loaded LDH-ME NPs@PC/ALG nanocomposite hydrogel beads at a comparable dosage of DOX. The nanocomposite hydrogel beads can release the drug in a time-dependent behavior, as discussed in section 3.1.6 of the study, which leads to a decrease in cytotoxicity. This aligns with similar observations reported in previous studies [20]. Due to the non-specific nature of DOX and the challenge of finding the right balance between a safe dose and effective concentration, it can result in severe side effects. Hence, a slower drug release rate can minimize these side effects, making it suitable for controlled and sustained delivery of anti-cancer drugs.

4. Conclusion

This work used a simple and environmentally friendly method to synthesize LDH-ME NPs@PC/ALG nanocomposite hydrogel beads. Ultimately, ME is a non-toxic, economical, and environmentally friendly chemical used in the green chemistry process to create LDH-ME NPs. Through the use of several techniques, including IR, XRD, SEM, and EDS, the structure of the synthesized nanocomposite hydrogel beads was examined and verified. Examining the antibacterial activity of LDH-ME NPS@PC/ALG nanocomposite hydrogel beads revealed their superior activity with 14- and 20-mm inhibition zones for *E. coli S. aureus*, respectively. The prepared nanocomposite hydrogel beads have a high DOX loading capacity (~92 %) and a pH-dependent release profile (low release rate, < 20 %, at pH 1.2 and controlled release rate, 89 %, at pH 7.4), which makes them a suitable system for targeted DOX delivery to colonic cancer cells. On the other hand, the ability of PC and ALG to block the release of DOX in the stomach's acidic environment is a result of their pH-sensitive swelling behavior. Additionally, *in-vitro* cytotoxicity data showed that whereas the blank nanocomposite has a high level of cytocompatibility (cell viability > 95 %), the prepared DOX-loaded LDH-ME NPs@PC/ALG nanocomposite hydrogel beads exhibit higher cytotoxicity (~13 % cell viability in 15.6 µg/mL) against HT-29 cells. These findings of the study thus highlight the potential of the hydrogel beads.

Roghayeh Fathi: Conceptualization, Methodology, Formal analysis, Investigation, Visualization, Software, Writing – Original Draft.

Siamak Javanbakht: Validation, Writing – Reviewing and Editing, Project administration

Reza Mohammadi: Resources, Validation, Writing – Reviewing and Editing, Supervision

CRediT authorship contribution statement

Roghayeh Fathi: Writing – original draft, Software, Methodology, Investigation, Formal analysis, Conceptualization, Visualization. **Siamak Javanbakht:** Writing – review & editing, Validation, Project administration. **Reza Mohammadi:** Writing – review & editing, Validation, Supervision, Resources.

Declaration of competing interest

The authors declare that they have no known competing financial interests or personal relationships that could have appeared to influence the work reported in this paper.

Acknowledgments

This research is supported by the research grant of the University of Tabriz (number SAD/2389-14020820).

Appendix A. Supplementary data

Supplementary data to this article can be found online at https://doi.org/10.1016/j.eurpolymj.2024.113548.

Data availability

Data will be made available on request.

References

[1] I. Gholamali, M. Yadollahi, Bio-nanocomposite polymer hydrogels containing nanoparticles for drug delivery: a review, Regener. Eng. Transl. Med. 7 (2021) 129–146.
[2] S. Rafieian, H. Mirzadeh, H. Mahdavi, M.E. Masoumi, A review on nanocomposite hydrogels and their biomedical applications, Sci. Eng. Compos. Mater. 26 (1) (2019) 154–174.
[3] J. Liu, X. Bao, I. Kolesnik, B. Jia, Z. Yu, C. Xing, J. Huang, T. Gu, X. Shao, A. Kletskov, Enhancing the in vivo stability of polycation gene carriers by using PEGylated hyaluronic acid as a shielding system, BIO Integration 3 (3) (2022) 103–111.
[4] X. Jing, H. Fu, B. Yu, M. Sun, L. Wang, Two-photon polymerization for 3D biomedical scaffolds: Overview and updates, Front. Bioeng. Biotechnol. 10 (2022) 994355.
[5] D.-Q. Li, M. Tohti, Y.-S. Fu, Y. Zhang, Z.-W. Xiong, J. Li, Y.-F. Guo, Aldehyde group pendant-grafted pectin-based injectable hydrogel, Int. J. Biol. Macromol. 264 (2024) 130453.
[6] J.-Q. Zhang, H.-C. Li, J. Wang, S.-S. Liu, J. Li, D.-Q. Li, Dopamine-functionalized pectin-based Pickering emulsion as an oral drug delivery system, Colloids Surf A Physicochem Eng Asp 673 (2023) 131807.
[7] S.-Y. Wang, M. Tohti, J.-Q. Zhang, J. Li, D.-Q. Li, Acylhydrazone-derived whole pectin-based hydrogel as an injectable drug delivery system, Int. J. Biol. Macromol. 251 (2023) 126276.

[8] M.T. Taghizadeh, H. Ashassi-Sorkhabi, R. Afkari, A. Kazempour, Cross-linked chitosan in nano and bead scales as drug carriers for betamethasone and tetracycline, Int. J. Biol. Macromol. 131 (2019) 581–588.
[9] H. Zhao, M. Liu, Y. Zhang, J. Yin, R. Pei, Nanocomposite hydrogels for tissue engineering applications, Nanoscale 12 (28) (2020) 14976–14995.
[10] K. Haraguchi, T. Takehisa, Nanocomposite hydrogels: A unique organic–inorganic network structure with extraordinary mechanical, optical, and swelling/de-swelling properties, Adv. Mater. 14 (16) (2002) 1120–1124.
[11] S. Merino, C. Martín, K. Kostarelos, M. Prato, E. Vázquez, Nanocomposite hydrogels: 3D polymer–nanoparticle synergies for on-demand drug delivery, ACS Nano 9 (5) (2015) 4686–4697.
[12] R. Gheorghita, L. Anchidin-Norocel, R. Filip, M. Dimian, M. Covasa, Applications of biopolymers for drugs and probiotics delivery, Polymers 13 (16) (2021) 2729.
[13] R.T. Ndebele, Q. Yao, Y.-N. Shi, Y.-Y. Zhai, H.-L. Xu, C.-T. Lu, Y.-Z. Zhao, Progress in the application of nano-and micro-based drug delivery systems in pulmonary drug delivery, BIO Integration 3 (2) (2022) 71–83.
[14] H. Wang, H. Fu, Y. Fu, L. Jiang, L. Wang, H. Tong, Z. Xie, P. Huang, M. Sun, Knowledge mapping concerning applications of nanocomposite hydrogels for drug delivery: a bibliometric and visualized study (2003–2022), Front. Bioeng. Biotechnol. 10 (2023) 1099616.
[15] V. Puri, A. Sharma, P. Kumar, I. Singh, Thiolation of biopolymers for developing drug delivery systems with enhanced mechanical and mucoadhesive properties: A review, Polymers 12 (8) (2020) 1803.
[16] J. Baranwal, B. Barse, A. Fais, G.L. Delogu, A. Kumar, Biopolymer: A sustainable material for food and medical applications, Polymers 14 (5) (2022) 983.
[17] G. Auriemma, A. Cerciello, R.P. Aquino, P. Del Gaudio, B.M. Fusco, P. Russo, Pectin and zinc alginate: the right inner/outer polymer combination for core-shell drug delivery systems, Pharmaceutics 12 (2) (2020) 87.
[18] A. Mohammadzadeh, S. Javanbakht, R. Mohammadi, Magnetic alginate core-shell nanoparticles based on Schiff-base imine bonding for pH-responsive doxorubicin delivery system, Colloids Surf A Physicochem Eng Asp (2024) 134473.
[19] L. Li, X. Zhang, X. Gu, S. Mao, Applications of natural polymeric materials in solid oral modified-release dosage forms, Curr. Pharm. Des. 21 (40) (2015) 5854–5867.
[20] H. Poursadegh, M.S. Amini-Fazl, S. Javanbakht, F. Kazeminava, Magnetic nanocomposite through coating mannose-functionalized metal-organic framework with biopolymeric pectin hydrogel beads: A potential targeted anticancer oral delivery system, Int. J. Biol. Macromol. 254 (2024) 127702.
[21] G. Viscusi, G. Gorrasi, Facile preparation of layered double hydroxide (LDH)-alginate beads as sustainable system for the triggered release of diclofenac: Effect of pH and temperature on release rate, Int. J. Biol. Macromol. 184 (2021) 271–281.
[22] J.P. Zanin, G.A. Gil, M.C. García, R. Rojas, Drug-Containing Layered Double Hydroxide/Alginate Dispersions for Tissue Engineering, ChemEngineering 6 (5) (2022) 70.
[23] Y. Luo, Q. Wang, Recent development of chitosan-based polyelectrolyte complexes with natural polysaccharides for drug delivery, Int. J. Biol. Macromol. 64 (2014) 353–367.
[24] M. Hiorth, T. Versland, J. Heikkilä, I. Tho, S.A. Sande, Immersion coating of pellets with calcium pectinate and chitosan, Int. J. Pharm. 308 (1–2) (2006) 25–32.
[25] T.W. Wong, S. Nurjaya, Drug release property of chitosan–pectinate beads and its changes under the influence of microwave, Eur. J. Pharm. Biopharm. 69 (1) (2008) 176–188.
[26] Y. Zhang, W. Wei, P. Lv, L. Wang, G. Ma, Preparation and evaluation of alginate–chitosan microspheres for oral delivery of insulin, Eur. J. Pharm. Biopharm. 77 (1) (2011) 11–19.
[27] S. Barkhordari, A. Alizadeh, Fabrication of pH-sensitive chitosan/layered double hydroxide (LDH)/Fe3O4 nanocomposite hydrogel beads for controlled release of diclofenac, Polym. Bull. 79 (7) (2022) 5533–5548.
[28] S. Mallakpour, M. Hatami, Fabrication and characterization of pH-sensitive bio-nanocomposite beads havening folic acid intercalated LDH and chitosan: drug release and mechanism evaluation, Int. J. Biol. Macromol. 122 (2019) 157–167.
[29] T. Xu, X. Xu, Y. Gu, L. Fang, F. Cao, Functional intercalated nanocomposites with chitosan-glutathione-glycylsarcosine and layered double hydroxides for topical ocular drug delivery, Int. J. Nanomed. (2018) 917–937.
[30] Y. Gu, C. Xu, Y. Wang, X. Zhou, L. Fang, F. Cao, Multifunctional nanocomposites based on liposomes and layered double hydroxides conjugated with glycylsarcosine for efficient topical drug delivery to the posterior segment of the eye, Mol. Pharm. 16 (7) (2019) 2845–2857.
[31] G. Mishra, B. Dash, S. Pandey, Layered double hydroxides: A brief review from fundamentals to application as evolving biomaterials, Appl. Clay Sci. 153 (2018) 172–186.
[32] A. Yadav, M. Pal, R.L. Goswamee, Biocompatible nanocomposite of carboxymethyl cellulose and functionalized carbon–norfloxacin intercalated layered double hydroxides, Carbohydr. Polym. 186 (2018) 282–289.
[33] T. Jeya Shree, V. Gowri Sree, S. Poompavai, E. Sieni, P. Sgarbossa, I. Camarillo, R. Sundararajan, Inhibition of proliferation of HeLa cells by pulsed electric field treated Mentha piperita (mint) extract, IETE J. Res. 68 (2) (2022) 858–868.
[34] N. Hudz, L. Kobylinska, K. Pokajewicz, V. Horčinová Sedláčková, R. Fedin, M. Voloshyn, I. Myskiv, J. Brindza, P.P. Wieczorek, J. Lipok, Mentha piperita: essential oil and extracts, their biological activities, and perspectives on the development of new medicinal and cosmetic products, Molecules 28 (21) (2023) 7444.
[35] R. Fathi, R. Mohammadi, Preparation of pH-responsive magnetic nanocomposite hydrogels based on k-carrageenan/chitosan/silver nanoparticles: Antibacterial carrier for potential targeted anticancer drug delivery, Int. J. Biol. Macromol. 246 (2023) 125546.
[36] S. Javanbakht, M. Shadi, R. Mohammadian, A. Shaabani, M.M. Amini, M. Pooresmaeil, R. Salehi, Facile preparation of pH-responsive k-Carrageenan/tramadol loaded UiO-66 bio-nanocomposite hydrogel beads as a nontoxic oral delivery vehicle, J. Drug Delivery Sci. Technol. 54 (2019) 101311.
[37] H. Jing, X. Huang, X. Du, L. Mo, C. Ma, H. Wang, Facile synthesis of pH-responsive sodium alginate/carboxymethyl chitosan hydrogel beads promoted by hydrogen bond, Carbohydr. Polym. 278 (2022) 118993.
[38] S.B. Nia, M. Pooresmaeil, H. Namazi, Carboxymethylcellulose/layered double hydroxides bio-nanocomposite hydrogel: A controlled amoxicillin nanocarrier for colonic bacterial infections treatment, Int. J. Biol. Macromol. 155 (2020) 1401–1409.
[39] T. Jeya Shree, V. Gowri Sree, S. Poompavai, E. Sieni, P. Sgarbossa, I. Camarillo, R. Sundararajan, Inhibition of proliferation of HeLa cells by pulsed electric field treated Mentha piperita (mint) extract, IETE J. Res. (2019) 1–11.
[40] V.A. Shirin, R. Sankar, A.P. Johnson, H. Gangadharappa, K. Pramod, Advanced drug delivery applications of layered double hydroxide, J. Control. Release 330 (2021) 398–426.
[41] S. Darvishi, S. Javanbakht, A. Heydari, F. Kazeminava, P. Gholizadeh, M. Mahdipour, A. Shaabani, Ultrasound-assisted synthesis of MIL-88 (Fe) coordinated to carboxymethyl cellulose fibers: A safe carrier for highly sustained release of tetracycline, Int. J. Biol. Macromol. 181 (2021) 937–944.
[42] S. Javanbakht, M. Nabi, M. Shadi, M.M. Amini, A. Shaabani, Carboxymethyl cellulose/tetracycline@ UiO-66 nanocomposite hydrogel films as a potential antibacterial wound dressing, Int. J. Biol. Macromol. 188 (2021) 811–819.
[43] H. Jafari, H. Namazi, pH-sensitive biosystem based on laponite RD/chitosan/polyvinyl alcohol hydrogels for controlled delivery of curcumin to breast cancer cells, Colloids Surf. B Biointerfaces 231 (2023) 113585.
[44] I. Braccini, S. Pérez, Molecular basis of Ca2+-induced gelation in alginates and pectins: the egg-box model revisited, Biomacromolecules 2 (4) (2001) 1089–1096.
[45] J. Li, Z.-L. Yang, T. Ding, Y.-J. Song, H.-C. Li, D.-Q. Li, S. Chen, F. Xu, The role of surface functional groups of pectin and pectin-based materials on the adsorption of heavy metal ions and dyes, Carbohydr. Polym. 276 (2022) 118789.
[46] A. Assifaoui, A. Lerbret, H.T. Uyen, F. Neiers, O. Chambin, C. Loupiac, F. Cousin, Structural behaviour differences in low methoxy pectin solutions in the presence of divalent cations (Ca 2+ and Zn 2+): A process driven by the binding mechanism of the cation with the galacturonate unit, Soft Matter 11 (3) (2015) 551–560.
[47] M. Arif, Z. Chi, Y.-J. Liu, C.-G. Liu, Preparation, characterization, and in vitro drug release behavior of thiolated alginate nanoparticles loaded budesonide as a potential drug delivery system toward inflammatory bowel diseases, J. Biomater. Sci. Polym. Ed. 31 (18) (2020) 2299–2317.
[48] M.B. Abd Elhaleem, A.A. Farghali, A.A. El-Shahawy, F.I.A. El-Ela, Z.E. Eldine, R. K. Mahmoud, Chemisorption and sustained release of cefotaxime between a layered double hydroxide and polyvinyl alcohol nanofibers for enhanced efficacy against second degree burn wound infection, RSC Adv. 10 (22) (2020) 13196–13214.
[49] K. Nakamoto, Infrared and Raman spectra of inorganic and coordination compounds, part B: applications in coordination, organometallic, and bioinorganic chemistry, John Wiley & Sons, 2009.
[50] A. Mohammadzadeh, S. Javanbakht, R. Mohammadi, F. Kazeminava, Ferrocene-functionalized magnetic core-shell nanoparticles based on hydrosilylation reaction for pH-responsive doxorubicin delivery system, Colloids Surf A Physicochem Eng Asp 703 (2024) 135201.